Dalton Transactions

ROYAL SOCIETY OF CHEMISTRY

PAPER

View Article Online
View Journal | View Issue

Check for updates

Cite this: *Dalton Trans.*, 2024, **53**, 2749

A mesoionic carbene stabilized nickel(II) hydroxide complex: a facile precursor for C–H activation chemistry†

Anna Pavun, Raffael Niess, Lucas A. Scheibel, Michael Seidl and Stephan Hohloch *

Received 9th November 2023,
Accepted 3rd January 2024

DOI: 10.1039/d3dt03746k

rsc.li/dalton

We report the synthesis of a new nickel(II) hydroxide complex **2** supported by a rigid, tridentate triazolylidene-carbazolid ligand. The complex can be accessed in high yields following a simple and stepwise extraction protocol using dichloromethane and aqueous ammonium chloride followed by aqeous sodium hydroxide solution. We found that complex **2** is highly basic, undergoing various deprotonation/desilylation reactions with E–H and C–H acidic and silylated compounds. In this context we synthesized a variety of novel, functionalized nickel(II) complexes with trimethylsilylolate (**3**), trityl sulfide (**4**), tosyl amide (**5**), azido (**6**), pyridine (**7**), acetylide (**8**, **9**), fluoroarene (**10** & **11**) and enolate (**12**) ligands. We furthermore found that **2** reacts with malonic acid dimethyl ester in a knoevennagel-type condensation reaction, giving access to a new enolate ligand in complex **13**, consisting of two malonic acid units. Furthermore, complex **2** reacts with acetonitrile to form the cyanido complex **14**. The formation of complexes **13** and **14** is particularly interesting, as they underline the potential of complex **2** in both C–C bond formation and cleavage reactions.

Introduction

Late transition metal hydroxides have been long proposed and identified to be crucial intermediates in a variety of biological and catalytic processes.[1,2–4] due to a rather weak metal hydroxide interaction.[2–4] Thus, in the past decades, they have emerged as valuable synthons in the preparation of novel and versatile functionalized metal complexes.[5–7] Nevertheless, due to the inherent weakness of the metal hydroxide interaction, the synthesis of terminal late transition metal hydroxide complexes still remains challenging.[8] Up to date, several examples of copper,[9–11] gold,[5,7] palladium[6,12] or platinum[13] complexes have been isolated,[14] which were found to be highly basic and show a large potential in insertion[11] and C–H activation chemistry[5,7] as well as catalysis.[10]

Contrasting these well explored examples, especially nickel-based hydroxide congeners have been less explored, despite nickel having a more pronounced oxophilicity. Initial reports of terminally bound hydroxides appeared in 2005 (please note that bridging hydroxide have been reported earlier[15]) when Campora and co-workers reported a new synthetic pathway replacing fluoride by lithium reagents, which, among others, gave access to the mononuclear nickel(II) hydroxide complex **A** (Fig. 1).[16] Alternatively, Mindiola and co-workers were able to access nickel(II) hydroxide complex **B** *via* an oxidative addition reaction using a low-valent nickel(I) precursor and water.[17] Using water as a synthon, in 2009, Zargarian deprotonated an nickel(II)-aqua complex to isolate complex **D**.[18] Similarly, Borovik and co-workers, reported the synthesis of complex **H**, which shows strong hydrogen bonding to the pending amidinate donors.[19] Similar hydrogen interactions were also found in the (yet only) NHC-stabilized nickel(II) hydroxide complex **J**, which has been shown to be valuable catalyst for Base-Free Michael reactions in air.[20] Asides from this catalytic application, the prevalent nickel(II) hydroxide complexes have mostly been studied towards their insertion reactivity. Due to the labile nature of the Ni–OH bond they easily insert various (polarized) molecules. For example the Piers group was able to show that complex **C** is an excellent catalyst for the hydration of nitriles to amines.[21] Similarly, the PN^3P supported complex **M** was also a versatile catalyst for this transformation. Other than that, various groups have shown, that nickel complexes **E**,[22] **F**,[23] **G**,[24] **M**,[25] and **K**[26] readily insert carbon monoxide,[24,25] carbon dioxide[22–26] and other cumulenes[25] to form the corresponding insertion products. Furthermore, Schneider and

Universität Innsbruck, Department of General, Inorganic and Theoretical Chemistry, Innrain 80–82, 6020 Innsbruck, Austria. E-mail: Stephan.Hohloch@uibk.ac.at

†Electronic supplementary information (ESI) available. CCDC 2294433–2294440, 2294579, 2294782, 2295617, 2296517 and 2306311. For ESI and crystallographic data in CIF or other electronic format see DOI: https://doi.org/10.1039/d3dt03746k

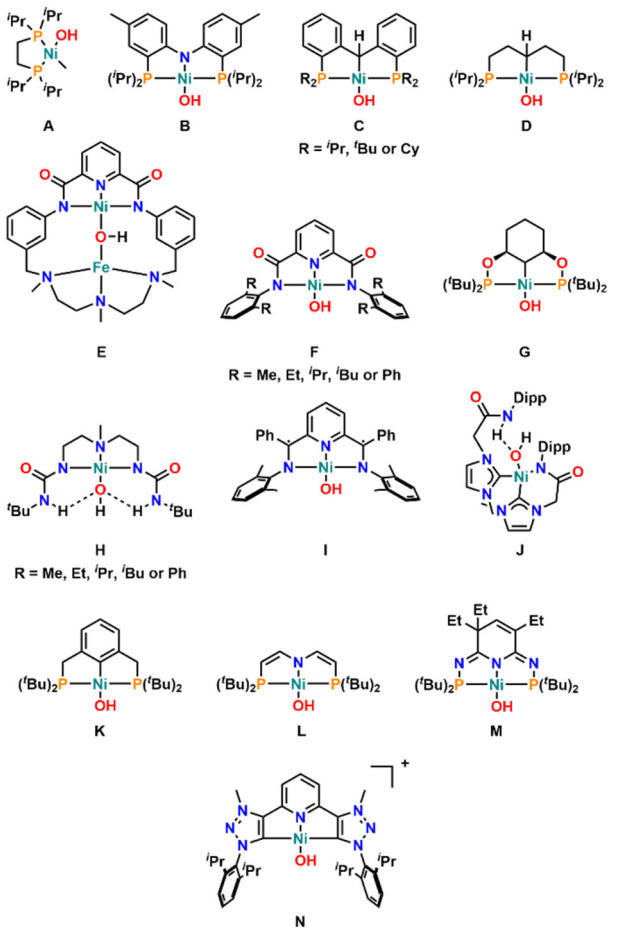

Fig. 1 Selected examples of nickel(II) and nickel(III) hydroxide complexes reported in the literature so far.

co-workers identified complex **L** as an intermediate in the photolytic insertion of CO_2 into nickel-hydride bonds, yielding the corresponding formiate complex as final product.[27] In addition, Matsubara and co-workers reported the bulky triazolylidene complex **N**, which is capable to deprotonate acetonitrile at the CH_3-group to stoichiometrically form a cyanomethyl ligand.[28] Notably, all these examples focus on the use of nickel(II) and yet only one nickel(III) hydroxide complex **I** has been isolated by Shanmugam *et al.*[29]

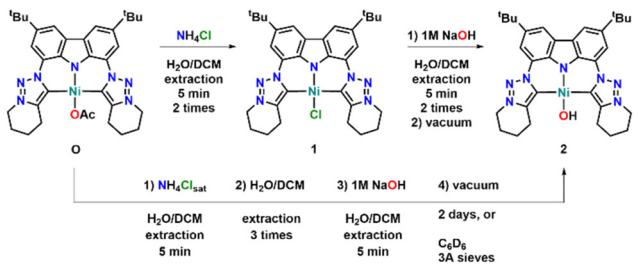

Scheme 1 Synthesis of the chloride complex **1** and subsequent derivatisation to the hydroxo complex **2**.

We have recently reported the synthesis of an *N*-fused tridentate carbazole-MIC ligand with intriguing properties in photochemistry[30] and the stabilisation of high-valent metal ions.[31] Furthermore, its nickel(II) acetate complex **O** (Scheme 1),[32] was found to be a versatile catalyst for the cyclisation of carbon dioxide and epoxide, while at the same moment being a bad catalyst for the corresponding polymerisation reaction. The latter has been actually a rare case where the use of a mesoionic carbene did not enhance the reactivity of a catalyst,[33] compared to its NHC analogue,[34] but instead lead to an inversion of selectivity. Here we expand the utility of the carbazole-MIC ligand further towards the stabilization of a rare, but readily accessible nickel(II) hydroxide complex *via* an acidic/basic work-up cascade starting from complex **O**. The complex was found to be a well-suited precursor for a large variety of protonolysis, CH-activation and insertion reactions, giving access to a wide array of functionalized metal complexes.

Results and discussion

Expanding our investigations in the reactivity of complex **O**, we found that in slightly acidic media facile exchange of the acetate ligand *versus* chloride is possible (Scheme 1). Indeed, already extracting/washing the crude acetate complex **O** with saturated ammonium chloride solution results in the formation of the brownish red chloride complex **1** in quantitative yields. Transformation of the acetate complex **O** into chloride complex **1** is evident by the absence of the methyl resonance at 1.96 ppm from the acetate group and by the general shift of the resonances in the aryl/alkyl region of the proton NMR spectra (compare Fig. S1 and S3†). The most striking difference here are the resonances in the aromatic region. In **O** these signals resonate as two singlets at 8.23 and 8.15 ppm, while in **1** they overlap to one singlet integrating to four protons at 8.17 ppm (Fig. S1 and S3†). Furthermore, the alkyl resonances are slightly broadened and no sharp multiplet analysis is possible anymore. Additionally, the presence of a resonance at 149.9 ppm in the ^{13}C-NMR spectrum of **1** unambiguously proves its assignment as a triazolylidene complex (Fig. S4†). Final proof of the formation of complex **1** was gained by X-ray diffraction analysis on single crystals obtained by slow evaporation of a concentrated dichloromethane solution at 0 °C (Fig. 2). This revealed a distorted square planar ligand environment around the nickel(II) center with a τ_4' parameter[35] of 0.27 in **1** *vs.* 0.07 in **O**. The metal nitrogen and carbene distances are thereby comparable to the acetate complex, and the chloride ligand is situated 2.2007(8) Å away from the nickel center, which is comparable to the literature. The relatively high τ_4' value results from a distortion of the chloride ligand out of the ligand-nickel plane by 1.125(2) Å, which was also found in other carbazolate derived nickel(II) complexes.[36]

Upon re-washing/extracting dichloromethane solutions of **1** with a 1 M NaOH solution (Scheme 1), we noticed a fast colour change from reddish-brown to dark red within the organic

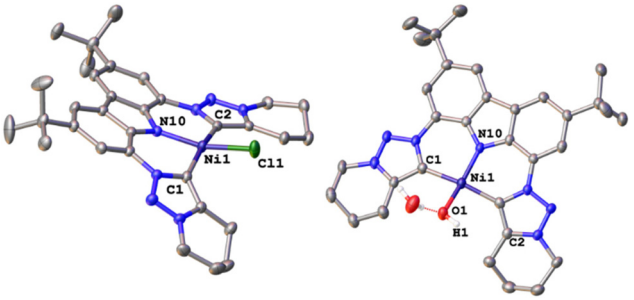

Fig. 2 Molecular structures of the chloride complex **1** and the water stabilized nickel(II) hydroxide complex **2[H_2O]**. Hydrogen atoms (except for ones being important in hydrogen interactions) and lattice solvent molecules have been omitted for clarity. Ellipsoids are shown at a probability level of 50%.

phase. Concentration of the organic phase and subsequent precipitation gave access to a dark red powder, which shows the presence of two different complexes in solution, which drastically differ from the starting chloride complex **1** (Fig. S9†). However, prolonged drying at elevated temperature (80 °C, two days) results in the formation of only one species (Fig. S8†) in the NMR. Interestingly, addition of a small drop of water, reforms the impurity observed in the original spectrum after workup, wherefore we attribute the two species to a "hydrated" form **2[H_2O]$_n$** (with an unknown amount of water, *vide infra*) and the non-hydrated hydroxide complex **2**. Alternatively, the hydroxide complex **2[H_2O]$_n$** can also be dried to give complex **2** by stirring a benzene solution with molecular sieves in the glovebox overnight. The absence of a characteristic triazolium resonance in the ^{1}H NMR as well as the presence of a triazolylidene resonance in its ^{13}C NMR spectrum at 168.5 ppm (Fig. S11†) being in the typical range for other nickel-triazolylidene complexes, proves the integrity of the CNC–Ni coordination framework in **2**. Unfortunately, neither NMR, nor IR gave conclusive proves for the presence of a OH ligand in the complex. Theoretical investigations showed, the OH-stretching frequency to appear at 3839 cm^{-1}, however no signal was detected there. We attribute this to the fact, that the hydroxide ligand can interact with small amounts of residual moisture in NMR solvents or ambient air (*vide infra*), which significantly broadens its resonances in the aforementioned spectroscopic techniques. However, unambiguous proof for the presence of a hydroxide ligand was delivered by X-ray diffraction studies on single crystals obtained by slow evaporation of a concentrated tetrahydrofuran solution at room temperature (Fig. 2). The analysis revealed, that the hydroxide ligand is additionally stabilized/coordinated *via* a strong hydrogen bond to a residual water molecule, most likely coming from "wet" crystallisation solvents. Therefore, the molecular composition in the crystal is best described as **2[H_2O]**. The hydrogen bond shows a distance of 1.885(4) Å (water to O1) and the Ni–OH distance was found to be 1.848(2) Å, which is comparable to other nickel(II) hydroxide complexes reported in the literature. Similar to the chloride complex **1**, the nickel center is in a distorted square planar environment, displaying a τ_4' value of 0.17. To check, whether the water arises from the crystallisation solvent, or from residual water in the sample, we have collected ^{1}H NMR data of single crystals in dry C_6D_6. The results clearly indicate, that the NMR spectra of **2** and **2[H_2O]** are identical (Fig. S10†), which can be explained by two reasons: In dry benzene, the water molecule from crystalline **2[H_2O]** is readily lost, giving access to the same NMR as observed for "dry" **2**, or the "dry" complex **2** contains a residual, unobservable water molecule. While an unambiguous assignment of these two cases is not possible, the observed protonolysis reactivity (*vide infra*) rather suggests the presence of a "water-free" hydroxide complex **2**. Notably, the hydroxide complex can also be directly accessed in a "one-pot" reaction starting from complex **O**. Double extraction of **O** with saturated NH_4Cl solutions, followed by three washings with deionized water and subsequent double extraction with 1 M NaOH also gives clean access to the hydroxide complex **2** after precipitation from DCM/hexane and drying under high-vacuum over two days. Alternatively, complex **2** can be obtained by drying a benzene solution of **2[H_2O]$_n$** over activated molecular sieves. This procedure gives a facile and simple access to the highly reactive hydroxide complex **2**. Although we do not have a crystal structure of the non—hydrated complex **2**, its follow-up reactivity is in line with the presence of a highly basic hydroxide ligand.

To further investigate the protonolysis reactivity of complex **2** we studied its reactivity to acidic E–H bonds (E = O, N, S) (Scheme 2). We found, that the complex readily reacts with alcohols, such as TMS-OH to give the dark red silenolate complex **3**. Furthermore, complex **2** reacts with triphenylthiomethanol (trityl-thiol) to give the thiotritylate complex **4** as well as with tosyl amine, to yield the tosyl amide complex **5**. Notably, all these complexes can also be accessed by the reaction of **1** with the corresponding alkali metal salts. However, the simplicity of the protonolysis route, using bottled reagents instead of moisture-sensitive alkali metal salts (being tedious to make) is a big advantage in accessing these functionalized complexes. Successful formation of the functionalized complexes **3–5** is evident by NMR spectroscopy, showing the resonances of the added ligands, as well as a distinct shift of the two aryl protons. However, the most striking feature, confirming the successful formation of the complexes, is found within the alkyl signals of the piperidyl-rings of the ligand, showing complicated multiplets instead of distinctive ones (Fig. S15, S20 and S25†). This indicates a strong steric hindrance within the complexes and a rigid orientation of the co-ligand. Indeed, crystal structure analysis (*vide infra*) supports a strong steric hindrance in these systems, allowing the additional ligand to adopt only one orientation (above or beneath the carbazole ligand plane) without an option to "swing through". The presence of a triazolylidene complex in **3–5** was furthermore confirmed by ^{13}C NMR spectroscopy, showing the characteristic resonances at 150.4, 150.1 and 149.3 ppm respectively (Fig. S16, S21 and S26†). Unambiguous proof for the formation of **3–5** was given by X-ray structure analysis. Single crystals suit-

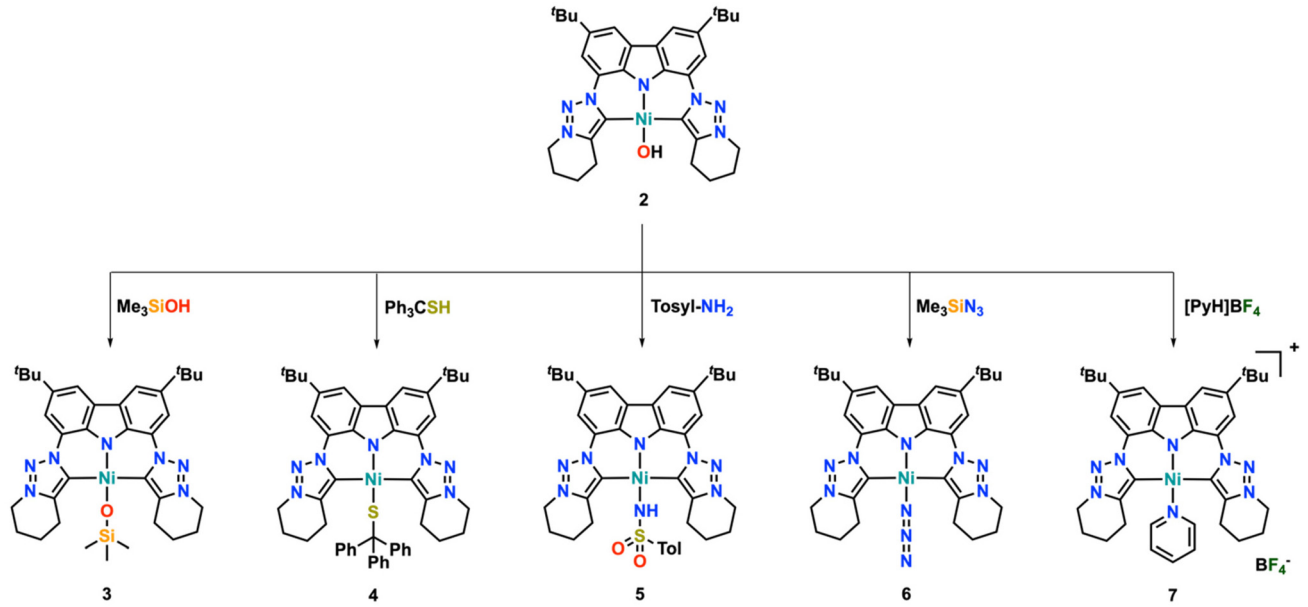

Scheme 2 Protonolysis reactivity of hydroxide complex **2** towards E–H acidic substrates leading to a variety of functionalized and cationic complexes.

able for X-ray diffraction were grown by vapor diffusion of pentane into a saturated dichloromethane solution for **3**, from a concentrated solution in toluene at −40 °C over 2 weeks for **4** and by slow evaporation of a concentrated benzene solution at room temperature for **5** (Fig. 3). The complexes crystallize in the triclinic space group $P\bar{1}$ along with one molecule of dichloromethane (for **3**) or in the monoclinic space group $P2_1/c$ with two molecules of toluene (for **4**) or one molecule of benzene (for **5**). Additionally, it is worth noting that the structural data of complex **4** shows a high extend of twinning which, unfortunately, is not well resolved. The complexes display Ni–carbene distances in the range of 1.906(10)–1.934 (4) Å and the nickel carbazole distance Ni1–N10 was found to lie in the range between 1.858(3)–1.892(9) Å for **3–5**. Notably, the longest metal ligand distances are found within complex **4**, which represents the steric bulk of the thiotrityl ligand quite well. The new co-ligands display a nickel – ligand distance of 1.874(3) Å for Ni1–O1 in **3**,[37] 2.243(6) Å for Ni1–S1 in **4**,[38] and 1.937(5) Å for Ni1–N40 in **5** [39] and are comparable to previously reported examples in the literature for these functionalities. All nickel complexes adopt a distortion from square planar which is reflected in relatively high τ_4' values of 0.16, 0.35 and 0.30 for **3**, **4** and **5** respectively.

Aside from the reaction with protic substrates, complex **2** also readily reacts with base-labile substrates such as TMS-azide to give the azido complex **6** as well as with protic salts, such as pyridinium tetrafluoroborate to give the cationic complex **7** (Scheme 2). Contrasting the complexes **3–5** the complexes **6** and **7** show discrete and well-defined multiplets in their ^{1}H NMR alkyl regions (Fig. S30 and S35–S37†), indicating (similar to **O**, **1** and **2**) a highly flexible nature of the co-ligands. The integrity of the triazolylidene ligand is proven by ^{13}C NMR spectroscopy, showing characteristic resonances at 145.4 (**6**) and 149.71 (**7**) ppm (Fig. S31 and S38†). The presence of tetrafluoroborate anion in **7** is confirmed by ^{19}F NMR spectroscopy, showing a singlet at −149.9 ppm (Fig. S39†). For complex **6**, the presence of an azido ligand is further indicated by the presence of a strong IR resonance at 2040 cm^{-1} being characteristic for metal-azido complexes (Fig. S89†). Unambiguous proof of the structural identity of the complexes **6** and **7** was given by X-ray diffraction analysis of single crystals grown by vapor diffusion of pentane into a concentrated dichloromethane solution for both, **6** and **7** (Fig. 3). Complex **6** crystallizes in the triclinic space group $P\bar{1}$ with one molecule of dichloromethane in the lattice, while the salt **7** was found to crystallize in the monoclinic space group $P2_1/c$ without any lattice solvent molecules. The nickel carbene distances Ni1–C1/Ni1–C2 are 1.954(5)/1.925(5) Å in **6** and 1.989(4)/1986(4) Å in **7**. The relatively long Ni1–C1/C2 distances in **7** can be explained by the fact, that this complex (together with complexes **10** and **11**, *vide infra*) displays the lowest distortion from the square planar ligand field (τ_4' = 0.04). Thus, the steric bulk of the pyridine elongates the nickel triazolylidene bonds compared to the other examples reported here. Unexpectedly, the nickel pyridine distance Ni1–N40 in **7** at 1.893(3) Å is shorter than the corresponding nickel nitrogen bond distances in the azido complex **6** (1.913(5) Å) and the tosylamide complex **5** (1.937(3) Å).

Having successfully proven, that the hydroxide complex **2** is actually a suitable precursor to deprotonate a large variety of E–H bonds, (Scheme 2) we turned our interest to less acidic substrates based on carbon (Scheme 3). Given the large potential of nickel in cross-coupling reactions,[40] the isolation and stability of complexes with a nickel–carbanion bond is highly

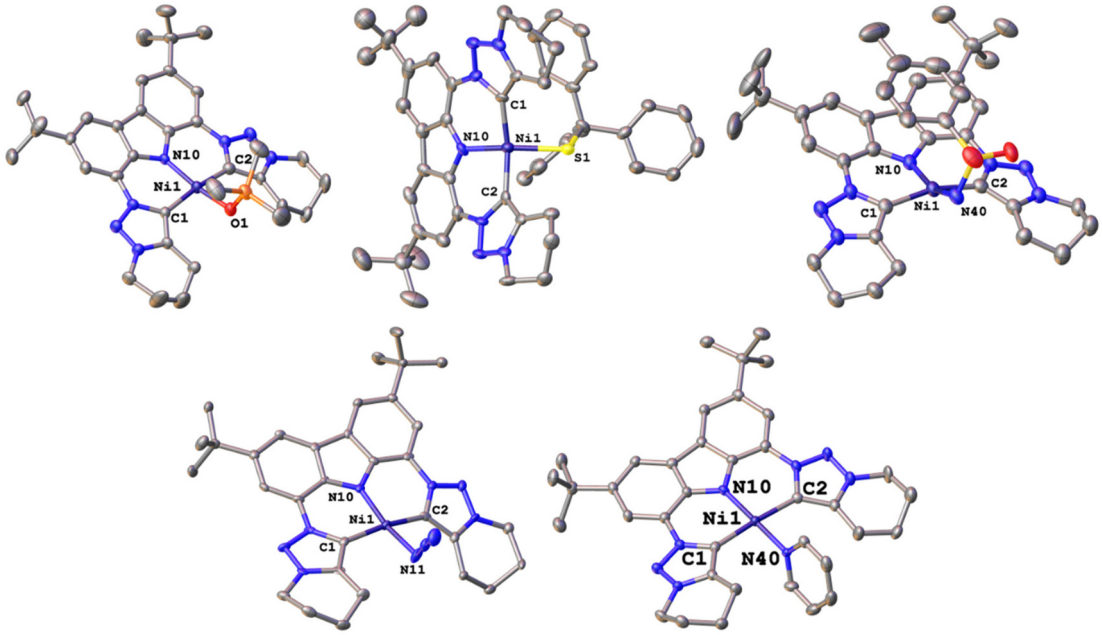

Fig. 3 Molecular structures of the nickel(II) complexes **3–5** (top) and **6** + **7** (bottom). Hydrogen atoms, counter ions and lattice solvent molecules have been omitted for clarity. Ellipsoids are shown at a probability level of 50%.

interesting. To initially attempt the probability to deprotonate C–H acidic substrates[41] we investigated the reactivity of **2** towards 3,5-bis-trifluoromethylphenylalkyne and 2,6-diisopropylphenyl-alkyne (Scheme 3). While at room temperature no obvious reaction progress was observed, elevated temperature of 50 °C (**8**) or 100 °C (**9**) lead to the clean deprotonation of the alkynes and the corresponding acetylide complexes **8** and **9** were isolated as dark red solids in yields of 99 and 73% respectively. Successful formation of the desired acetylide complexes is indicated by several observations from their ^{1}H NMR spectra, *e.g.* the presence of the aryl signals (Fig. S43 and S49†) and the absence of the terminal CH resonance of the corresponding alkynes (3.26 ppm for 3,5-bis(trifluoromethyl)-phenylalkyne and 3.51 ppm for 2,6-diisopropylphenylalkyne). Furthermore, the presence of a new ^{13}C NMR resonance at 114.3 and 113.8 ppm for **8** and **9** corresponding to the nickel bound acetylide carbon atom (Fig. S44 and S50†). In addition, the ^{13}C NMR resonances at 152.5 (**8**) and 153.1 ppm (**9**) are a proof for an intact triazolylidene complex of nickel(II). Finally, the shift of the ^{19}F-NMR resonances from −63.3 ppm in free 3,5-bis(trifluoro-methyl)phenylalkyne to −62.8 ppm in complex **8** is a useful indicator that the electronic situation of the alkyne has changed (Fig. S45†). Unambiguous proof for the formation of the anticipated acetylide complexes was given by X-ray diffraction analysis of single crystals grown from a cold (−40 °C) solution of **8** in toluene or by vapor diffusion of pentane into a concentrated benzene solution of **9** (Fig. 4). Both complexes crystallize as solvates in the triclinic or monoclinic space groups $P\bar{1}$ or $P2_1/c$. Independent of the electronic substitution of the phenyl ring in **8** and **9**, the nickel–acetylide distance Ni1–C40 was found to be identical displaying bond lengths of 1.846(4) and 1.849(4) Å respectively and compare well with previously characterized nickel(II)–acetylide complexes.[42] In line with the steric repulsion of the 2,6-diisopropyl substitution pattern *vs.* the 3,5-bis(trifluoromethyl) the nickel carbene distances Ni1–C1 and Ni1–C2 are slightly longer in **9** compared to **8** (1.947(4) *vs.* 1.913(4) Å and 1.938(4) *vs.* 1.914(4) Å). Similar to the other (bulkier) co-ligands examined above, the acetylide ligands are shifted out-of-plane, resulting in a slight deviation of the expected square planar ligand environment around nickel(II) (τ_4 = 0.26 for **8**; 0.16 for **9**).

Moving to more challenging substrates, we next investigated the direct deprotonation of tetrafluoro- and pentafluoro-benzene (Scheme 3). Similar to the acetylenes, no reaction was observed at room temperature, however at 120 °C the reactions proceed slowly when a threefold excess of the corresponding fluoroarene is used. We found that scaling of both deprotonations is not feasible, however, in well-concentrated NMR reactions the product formation can be monitored and full conversion is achieved after six days and the complexes can be cleanly isolated after work-up. Successful formation of the desired pentafluoro- and tetrafluorophenyl complexes **10** and **11** is indicated by ^{19}F NMR spectroscopy, showing three signals for **10** at −111.2, −163.1 and −164.9 ppm (Fig. S56†) differing drastically from free C_6F_5H (−139.2, −154.3, −162.6 ppm) and two signals at −113.3 and −142.8 ppm for **11** (Fig. S62†). Especially in the latter case, the splitting of the ^{19}F resonance into two multiplets is characteristic for the coordination of the tetrafluorobenzene towards a metal center. Additional proof is given by ^{1}H NMR spectroscopy showing no remaining C–H arene signal for pentafluorobenzene at 5.90 ppm in **10** (Fig. S54†) and one

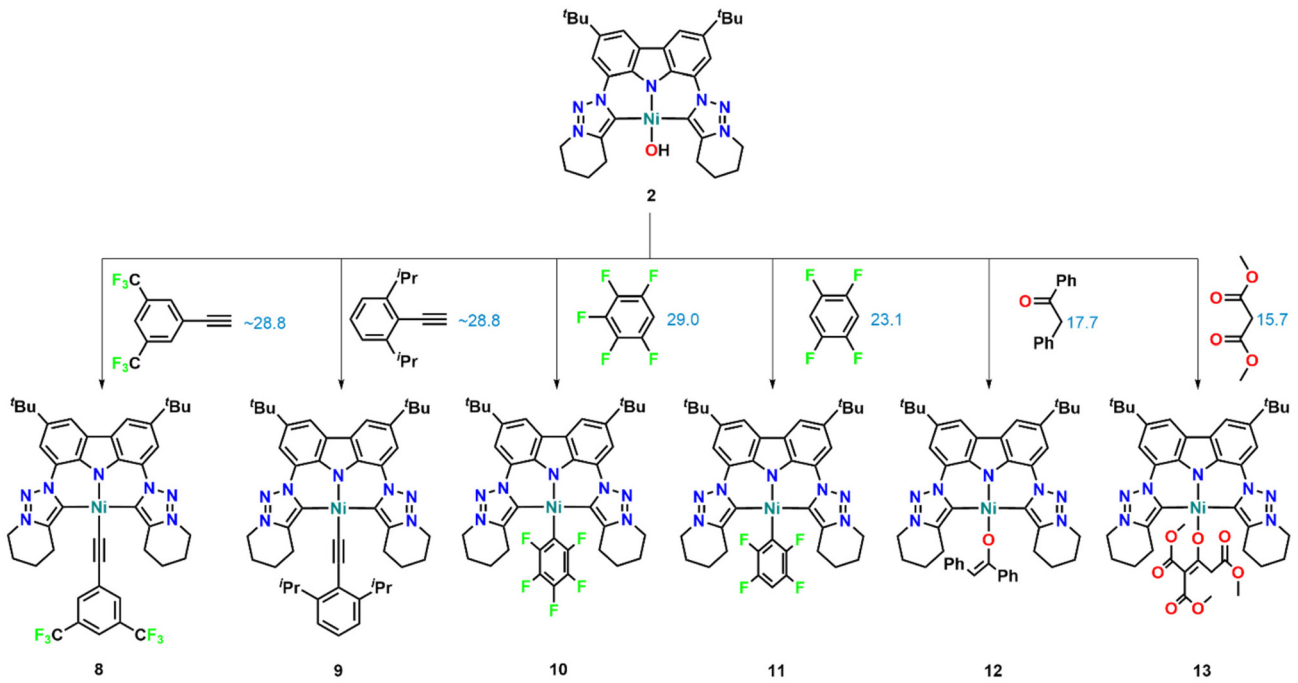

Scheme 3 C–H activation chemistry of selected C–H acidic substrates with the hydroxide complex **2**. The blue values indicate the pK_a value of the most acidic proton in DMSO taken from ref. 41.

multiplet at 6.74 ppm corresponding to the *para*-H of the tetrafluorophenyl ligand in **11** (Fig. S60†). This is also substantially different from free tetrafluorobenzene (6.28 ppm). Furthermore, ^{13}C NMR spectroscopy proofed the presence of a triazolylidene species, displaying the characteristic resonances at 149.2 and 149.6 ppm for **10** and **11** respectively (Fig. S55 and S61†). X-ray diffraction analysis of crystals grown by slow evaporation of a benzene solution of **11** at room temperature unambiguously proofed the presence of the desired fluoroarene complexes (Fig. 4). Unfortunately, for complex **10** no crystals suitable for X-ray diffraction analysis have been obtained under any conditions tried. Complex **11** crystallizes in the triclinic system ($P\bar{1}$) with 0.8 eq. of benzene. As expected, the nickel center adopts a square planar coordination environment, displaying τ_4' value 0.04. The nickel carbon distances Ni1–C40 to the fluoroarene ligand was found to be 1.867(4) Å. This nickel–carbon distances compare well to other structurally characterized tetrafluorophenyl-[43–46] and pentafluorophenyl[15,47] complexes of nickel previously reported. Notably, the Ni1–C40 distances are slightly longer (*ca.* 0.05 Å) compared to the acetylide species **8** and **9** (*vide supra*) which reflects the larger steric crowding within the fluoroarene complex **11**. Furthermore, the nickel triazolylidene distances were found to be 1.972(4) and 1.977(4) Å for **11** and are significantly longer compared to the nickel–arene distances Ni1–C40. It is worth mentioning at this point that the majority of tetrafluorophenyl- and pentafluorophenyl complexes of nickel (*vide supra*) have been accessed by oxidative insertion of low-valent nickel precursors into C–F [43,46,48] and C–H bonds[45,49] or through salt metathesis routes using Grignard reagents,[15] rather than through a deprotonative strategy as described here.

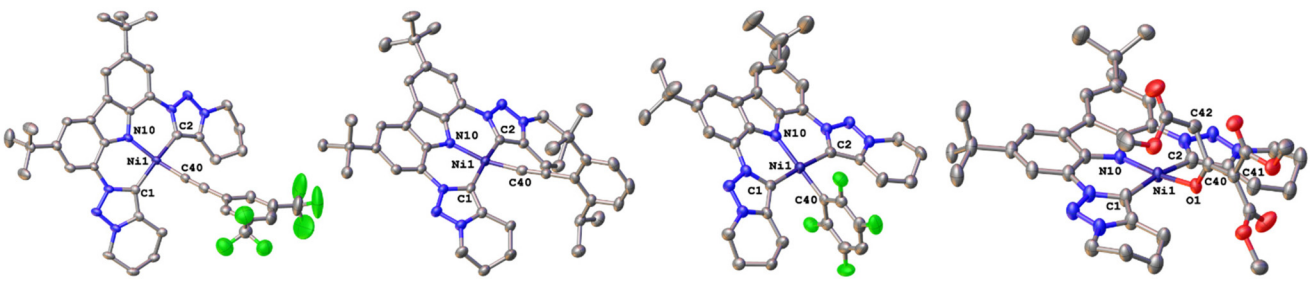

Fig. 4 Molecular structures of the C–H activated complexes **8**, **9**, **11** and **13** (from left to right). Hydrogen atoms and lattice solvent molecules have been omitted for clarity. Ellipsoids are shown at a probability level of 50%.

Showing that we can deprotonate a variety of pure carbon centred substrates, we choose to investigate "ambivalent" substrates next, which can coordinate either *via* a C-terminus or and O-terminus after deprotonation at an activated CH_2 group. For this purpose, we chose 1,2-diphenylethanone and dimethyl malonic ester (Scheme 3). Depending on the metal centre used, both substrates have shown to either coordinated *via* the C-[5,50] or *via* the O-donor[51] atom after deprotonation. Both substrates required temperatures of 120 °C for two days (**12**) and two hours (**13**) to completely convert to the new products. The ^{1}H NMR spectrum of **12** shows a characteristic resonance at 5.91 ppm (Fig. S66†) corresponding to the remaining proton on the α-carbon next to the carbonyl group. Bochmann and co-workers recently reported a C-bound di-phenylethanone at a gold(I) center, in which this proton was found at δ = 4.80 ppm.[5] Despite discussing different metals here, the shift of about 1 ppm in nickel *vs.* gold is already indicative, that the diphenylethanone is bound *via* the O-donor towards the nickel atom, adopting an enolate configuration. In addition, several multiplets corresponding to phenyl groups are present in the ^{1}H NMR spectrum of **12**. Unfortunately, despite several attempts, only strongly twinned crystals could be grown of the complexes and the obtained X-ray data did not allow a sufficient refinement of the structure, which resulted in high *R*-values. Nevertheless, the solution unambiguously allowed to determine the connectivity and the model as such is reliable, despite no bond distances can be discussed. The structural connectivity (Fig. S113†) unambiguously proves the presence of an enolate ligand being bond to the nickel(II) center. Interestingly, if the reaction between desoxybenzoin (1,2-diphenylethan-1-one) and complex **2** is performed under air, instead of argon, a complex mixture of products is obtained (Fig. S72†), from which the benzoate complex **12′** could be crystallized in minimal quantities (Fig. S71 and S112†). Notably, the nickel- and base-mediated oxidation of benzoin-derivatives[52] in the presence of oxygen has been previously reported and is an indication, that beyond the stoichiometric activation of C–H bonds, complex **2** could also be a potent oxygenation catalyst under the right conditions.

Contrasting for the expected malonate complex the ^{1}H NMR revealed some unexpected features (Fig. S73†): the most striking one, is the presence of three methoxy resonances at 3.77, 3.51 and 3.04 ppm each integrating to three protons. The second unexpected observation, was the presence of a singlet at 6.08 ppm integrating to two protons. This resonance corresponds to the hydrogen atoms attached to the α-carbon, positioned between the carboxy groups. The assignment of this resonance has been unambiguously proven by ^{1}H–^{13}C HSQC and Dept 135 ^{13}C NMR spectroscopy (Fig. S77 and S75†) with the latter showing a negative peak at 49.8 ppm corresponding to the α-carbon atom. Given the fact that these hydrogen atoms on the α-carbon are the most acidic protons in malonic acid dimethyl ester, the integrity of the CH_2 group after the reaction is highly surprising and suggests that something else than a simple deprotonation reaction must have occurred. To answer this question, we were able to obtain X-ray quality crystals of **13** by slow evaporation of a concentrated diethyl ether solution at room temperature. Although these crystals contained about 12% of **1** as an impurity (Fig. S114†), most likely being present due to DCM contamination during the crystallisation process, *vide infra*, X-ray diffraction analysis of these crystals indeed confirmed the presence of an unexpected Knoevennagel addition product at the malonate ligand (Fig. 4, left). In fact, two equivalents of malonic acid dimethyl ester participate in the reaction to give a new 1,5-dimethoxy-2-(methoxycarbonyl)-1,5-dioxopent-2-en-3-olate ligand at the nickel center. Scheme 4 shows a putative mechanism how the enolate ligand might be forming. The enolate-form is unambiguously confirmed from the C40–C41 distance, being 1.395 (5) Å. The nickel oxygen distance Ni1–O1 was found to be 1.913(2) and is therefore slightly longer compared to the siloxide complex **3** (1.874(3) Å, *vide supra*) or the acetate complex **O** (1.878(1) Å)[32] but comparable to the benzoate complex **12′** (1.906(3) Å, see ESI, Tables S1–S4 and Fig. S112†). Asides, all other bond metrics are in agreement with the other examples discussed within here. Notably, the corresponding alcohol of the condensation product ion **13** has already been reported in 1910,[53] but since then no other example has been reported.

Finally, we found that complex **2** is highly sensitive towards the reaction solvents used. For example, addition of dichloromethane to solutions of **2** reforms the chloride complex **1** within hours. While this is somewhat expected, surprisingly, complex **2** also reacts with acetonitrile to form the cyanide complex **14** (Scheme 5). This is unexpected, as previously reported nickel-hydoxide complex **N** was found to deprotonate

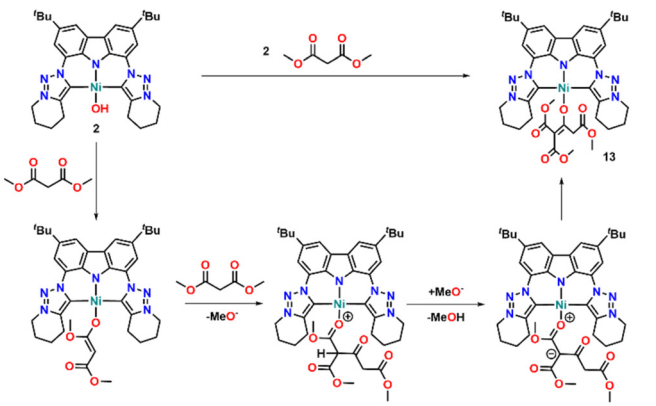

Scheme 4 Proposed mechanism for the formation of complex **13** *via* a Knoevenagel-type condensation reaction.

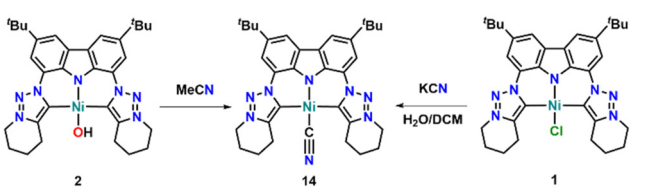

Scheme 5 Synthetic strategies towards the cyanido complex **14** starting from the hydroxo complex **2** or the chloride complex **1**.

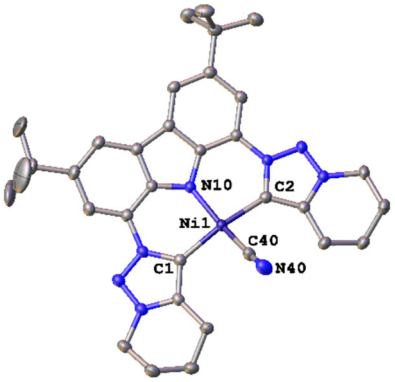

Fig. 5 Molecular structure of the cyanido complex **14**. Hydrogen atoms have been omitted for clarity. Ellipsoids are shown at a probability level of 50%.

MeCN at the CH_3-group forming the corresponding cyanomethyl complex.[28] Furthermore, the hydroxide complexes **C** and **M** were both studied towards their catalytic potential to catalyse the hydration of nitriles to amines[21,25] and **M** also stoichiometrically reacts with MeCN to form the corresponding acetamide complex.[25] Thus, the cleavage of the C–C bond in MeCN was quite unexpected but is not unprecedented as was shown by Zhang and co-workers, who reported the *in situ* cleavage of MeCN during the synthesis of nickel(II)-NHC complexes from imidazolium salts, nickel acetate and NaH/KO^{t}Bu mixtures.[54] Mechanistic studies towards this activation reaction are still ongoing, however, form *in situ* experiments in MeCN-d_3, we can yet confidently say that σ-bond metathesis to form methanol as a second product is not occurring and a more complex reaction mechanism must be present here. Notably, complex **14** can also be synthesized, by washing complex **1** in dichloromethane with an aqueous potassium cyanide solution. The presence of the cyanide ligand in complex **14** was evident by the presence of a strong IR band at 2107 cm^{-1} (Fig. S97†). This value is shifted compared to free KCN (2075 cm^{-1}, Fig. S98†) but lies in the range of other reported cyanide complexes (2109 cm^{-1} or 2108 cm^{-1}).[54,55] Nevertheless, X-ray diffraction analysis of single crystals grown by slow evaporation of a MeCN solution of complex **14** unambiguously confirmed the presence of the cyanide ligand (Fig. 5), displaying a Ni1–C40 distance of 1.8501(18) Å. With a C40–N40 distance of 1.147(2) Å within the cyanide ligand, these bond metrics fit well with previously reported (NHC)–nickel(II) cyanide complexes.[54,55] Further investigations to utilize the C–C bond activation reactivity of complex **2** are still ongoing.

Conclusions

In conclusion we have reported the facile access to a highly reactive nickel(II) hydroxide complex, which is a potent and useful precursor for the synthesis of highly functionalized nickel(II) complexes. We have shown that the complex is capable to deprotonate a variety of E–H acidic compounds such as alcohols, thiols and amides as well as C–H acidic substrates such as alkynes, fluoroarenes and C–H conjugated substrates such as ethanone or malonic acid ester. The latter activation reaction revealed the rare formation of a Knoevenagel-type condensation product leading to the formation of complex **13**. Despite this reaction was unexpected in the first place, it shows the potential of complex **2** to also engage in complex C–C bond formation reactions, as the observed enolate has not been reported in the past 100 years. Furthermore, we present first results that the complex can also be used to desilylate TMS-protected substrates such as TMS-azide. Furthermore complex **2** is also capable of cleaving C–CN bonds as the one in acetonitrile. With these examples in hand, the presented hydroxide complex **2** can be viewed as a valuable synthon in late transition metal chemistry and a rich and versatile follow-up chemistry of the presented molecules can be expected.

Experimental section

Materials and methods

If not otherwise mentioned, all transformations involving nickel precursors were carried out under inert conditions using the Schlenk technique or an argon-filled glovebox. Organic syntheses were carried out under ambient conditions without taking precautions to exclude moisture or air. Solvents were dried by a MBraun SPS system and stored over activated molecular sieves (3 Å) for at least 24 h. The deuterated solvents C_6D_6, CD_2Cl_2 and C_5D_5N were degassed (purging with argon for 15 minutes) and dried over molecular sieves (3 Å) for at least 24 hours. All other chemicals were used as received without any further precautions being taken. Complex **O** was synthesized as previously reported.[32] IR spectra were recorded at room temperature under inert conditions using a Bruker Alpha 1 with ATR equipment. UV-Vis spectra were recorded using a Avantes spectrometer quipped with an deuterium and halogen light source and a CMOS detector (300–1700 nm). NMR spectra were collected at 298 K on a Bruker AV-400 using J-Young NMR tubes. All chemical shifts (δ) are reported in ppm. ^{1}H and ^{13}C chemical shifts were calibrated to residual solvent peaks. ^{19}F chemical shifts were referenced *vs.* $CFCl_3$.

Synthetic procedures

(3,6-Di-*tert*-butyl-1,8-bis-(2,4,5,6-tetrahydropyridin-1,2,3-triazolylidene)-carbazolid) nickel(II) chloride (1). A solution of **O** (1.00 g, 1.57 mmol) in dichloromethane (80 mL) was extracted with saturated ammonium chloride solution twice, immediate colour change from red to dark brown was observed. The organic phase was dried over sodium sulfate and concentrated *in vacuo.* The addition of *n*-hexane led to precipitation of **1**, which was isolated by filtration and dried in air to give **1** as brown powder quantitively (963 mg, 1.57 mmol). ^{1}H NMR (C_6D_6, 298 K, 400 MHz, in ppm): 8.54 (s, 2H, Aryl–H), 8.48 (s, 2H, Aryl–H), 3.65 (t, J = 6.4 Hz, 4H, CH_2), 3.37 (s, 4H, N–CH_2),

1.56 (s, 18H, $C(CH_3)_3$), 1.23 (s, 4H, CH_2), 1.02 (s, 4H, CH_2); $^{13}C\{^1H\}$ NMR (C_6D_6, 298 K, 101 MHz, in ppm): 149.9 (triazolylidene), 145.6 (Aryl–C), 141.5 (Aryl–C), 140.1 (Aryl–C), 138.5 (Aryl–C), 124.1 (Aryl–C), 116.9 (Aryl–CH), 111.7 (Aryl–CH), 47.4 (N–CH_2), 35.1 ($C(CH_3)_3$), 32.5 ($C(CH_3)_3$), 26.0 (CH_2), 21.7 (CH_2), 20.1 (CH_2). Elemental analysis calcd for $C_{32}H_{38}N_7Cl_1Ni_1 \cdot 1.6\ CH_2Cl_2$ (%) C 53.76 H 5.53 N 13.06 found C 53.52 H 5.58 N 13.43.

(3,6-Di-*tert*-butyl-1,8-bis-(2,4,5,6-tetrahydropyridin-1,2,3-triazolylidene)-carbazolid) nickel(II) hydroxide (2). A solution of **1** (500 mg, 0.813 mmol) in dichloromethane (50 mL) was extracted with two portions of sodium hydroxide solution (1 M, 30 mL) and two portions of water (30 mL). The bright red organic phase was dried over sodium sulfate and concentrated *in vacuo.* The addition of *n*-hexane led to precipitation of **2**, which was collected by filtration and dried *in vacuo* at 80 °C to give **2** as dark red powder in a yield of 93% (451 mg, 0.756 mmol). ^1H NMR (C_6D_6, 298 K, 400 MHz, in ppm): 7.93 (s, 2H, Aryl–H), 7.91 (s, 2H, Aryl–H), 3.82 (m, 2H, N–CH_2), 3.60 (m, 2H, CH_2), 3.43 (m, 4H, N–CH_2, CH_2), 1.67 (s, 18H, $C(CH_3)_3$), 1.51 (m, 4H, CH_2), 1.26 (m, 4H, CH_2); $^{13}C\{^1H\}$ NMR (C_6D_6, 298 K, 101 MHz, in ppm): 168.5 (triazolylidene), 150.3 (Aryl–C), 145.7 (Aryl–C), 138.0 (Aryl–C), 137.4 (Aryl–C), 123.0 (Aryl–C), 116.5 (Aryl–CH), 110.3 (Aryl–CH), 47.7 (N–CH_2), 35.0 ($C(CH_3)_3$), 32.8 ($C(CH_3)_3$), 24.4 (CH_2), 22.1 (CH_2), 20.3 (CH_2).

(3,6-Di-*tert*-butyl-1,8-bis-(2,4,5,6-tetrahydropyridin-1,2,3-triazolylidene)-carbazolid) nickel(II) trimethylsilanolate (3). To a suspension of **2** (20.0 mg, 33.5 μmol, 1 equiv.) in pentane (5 mL) molecular sieves and trimethyl silanol (30.2 mg, 335 μmol, 10 equiv.) were added. The mixture was stirred at room temperature in an argon atmosphere for 48 h to give a light red solution. The mixture was filtrated, and all volatiles were removed *in vacuo*. The resulting light red solid was redissolved in pentane and filtrated again. Removal of the solvent *in vacuo* yielded 67% (15.0 mg, 33.5 μmol) of **3** as light red powder. ^1H NMR (CD_2Cl_2, 298 K, 400 MHz, in ppm): 8.17 (d, J = 1.8 Hz, 2H, Aryl–CH), 8.11 (d, J = 1.8 Hz, 2H, Aryl–CH), 4.54 (m, 2H, N–CH_2), 4.42 (m, 2H, N–CH_2), 3.45 (m, 2H, CH_2), 3.25 (m, 2H, CH_2), 2.20 (m, 2H, CH_2), 2.12 (s, 2H, CH_2), 2.01 (m, 2H, CH_2), 1.86 (m, 2H, CH_2), 1.50 (s, 18H; $C(CH_3)_3$), −0.18 (s, 9H, TMS–CH_3); $^{13}C\{^1H\}$ NMR (CD_2Cl_2, 298 K, 101 MHz, in ppm): 150.4 (triazolylidene), 145.8 (Aryl–C), 139.9 (Aryl–C), 127.5 (Aryl–C), 125.6 (Aryl–C), 123.5 (Aryl–C), 116.5 (Aryl–CH), 111.0 (Aryl–CH), 48.5 (N–CH_2), 35.2 ($C(CH_3)_3$), 32.4 ($C(CH_3)_3$), 25.0 (CH_2), 22.8 (CH_2), 20.7 (CH_2), 4.1 (TMS–CH_3).

(3,6-Di-*tert*-butyl-1,8-bis-(2,4,5,6-tetrahydropyridin-1,2,3-triazolylidene)-carbazolid) nickel(II) tritylthiolate (4). To a solution of **2** (20.0 mg, 33.5 μmol, 1 equiv.) in toluene (3 mL) solid triphenylmethanethiol (11.1 mg, 40.2 μmol, 1.2 equiv.) was added at room temperature under air, immediate colour change from red to brown was observed. Removal of all volatiles *in vacuo* and washing the remaining solid with *n*-hexane twice gave **4** as orange powder in quantitative yields. ^1H NMR (CD_2Cl_2, 298 K, 400 MHz, in ppm): 8.18 (d, J = 1.7 Hz, 2H, Aryl–H), 8.01 (d, J = 1.7 Hz, 2H, Aryl–H), 7.48 (m, 6H, Trit-H), 6.76 (m, 3H, Trit-H), 6.65 (m, 6H, Trit-H), 4.40 (m, 4H, N–CH_2), 3.82 (m, 2H, CH_2), 3.39 (m, 2H, CH_2), 2.17 (m, 4H, CH_2), 2.09 (m, 2H, CH_2), 1.93 (m, 2H, CH_2), 1.55 (s, 18H, $C(CH_3)_3$); $^{13}C\{^1H\}$ NMR (CD_2Cl_2, 298 K, 101 MHz, in ppm): 150.5 (Trit-C), 150.1 (triazolylidene), 144.9 (Aryl–C), 140.0 (Aryl–C, 138.8 (Aryl–C), 130.3 (Trit-CH), 127.2 (Aryl–C), 126.2 (Trit-CH), 124.7 (Trit-CH), 123.9 (Aryl–C), 116.5 (Aryl–CH), 111.5 (Aryl–CH), 65.1 (Trit-C), 48.2 (N–CH_2), 35.3 ($C(CH_3)_3$), 32.4 ($C(CH_3)_3$), 24.8 (CH_2), 22.8 (CH_2), 20.6 (CH_2).

(3,6-Di-*tert*-butyl-1,8-bis-(2,4,5,6-tetrahydropyridin-1,2,3-triazolylidene)-carbazolid) nickel(II) tosylamide (5). A solution of **2** (40.0 mg, 67.1 μmol, 1 equiv.) in toluene (5 mL) was treated with *p*-toluenesulfonamide (11.5 mg, 67.1 μmol, 1 equiv.) at room temperature under air to give a dark red solution. Removal of the solvent *in vacuo* and washing the remaining solid with *n*-hexane gave **5** as orange to red powder in a yield of 75% (33.1 mg, 50.3 μmol). ^1H NMR (C_6D_6, 298 K, 400 MHz, in ppm): 8.52 (d, J = 1.7 Hz, 2H, Aryl–H), 8.46 (d, J = 1.7 Hz, 2H, Aryl–H), 8.28 (d, J = 8.1 Hz, 2H, Tos-H), 6.36 (d, J = 7.9 Hz, 2H, Tos-H), 3.51 (m, 2H, N–CH_2), 3.36 (m, 2H, CH_2), 3.27 (m, 2H, N–CH_2), 3.18 (m, 2H, CH_2), 1.73 (s, 3H, Tos-CH_3), 1.56 (s, 18H, $C(CH_3)_3$), 1.42 (m, 4H, CH_2), 1.07 (m, 4H, CH_2); $^{13}C\{^1H\}$ NMR (C_6D_6, 298 K, 101 MHz, in ppm): 149.3 (triazolylidene), 147.3 (Tos-C), 144.1 (Aryl–C), 140.0 (Aryl–C), 138.6 (Aryl–C), 138.5 (Tos-C), 128.6 (Aryl–C), 127.9 (Tos-CH), 126.5 (Tos-CH), 123.9 (Aryl–C), 117.0 (Aryl–CH), 111.5 (Aryl–CH), 47.4 (N–CH_2), 35.1 ($C(CH_3)_3$), 32.5 ($C(CH_3)_3$), 24.9 (CH_2), 21.6 (CH_2), 21.0 (Tos-CH_3), 20.0 (CH_2).

(3,6-Di-*tert*-butyl-1,8-bis-(2,4,5,6-tetrahydropyridin-1,2,3-triazolylidene)-carbazolid) nickel(II) azide (6). A solution of **2** (40.0 mg, 67.1 μmol, 1 equiv.) in dichloromethane (5 mL) was treated with trimethylsilyl azide (10.8 mg, 93.9 μmol, 1.4 equiv.) at room temperature under air. After stirring for five minutes, removal of all volatiles *in vacuo* gave **6** as orange powder in quantitative yields. ^1H NMR (CD_2Cl_2, 298 K, 400 MHz, in ppm): 8.25 (d, 2H, Aryl–H, J = 1.8 Hz), 8.17 (d, 2H, Aryl–H, J = 1.8 Hz), 4.52 (t, 4H, CH_2, J = 6.3 Hz), 3.42 (t, 4H, CH_2, J = 6.4 Hz), 2.21 (m, 4H, CH_2), 2.02 (m, 4H, CH_2), 1.51 (s, 18H, $C(CH_3)_3$); $^{13}C\{^1H\}$ NMR (CD_2Cl_2, 298 K, 101 MHz, in ppm): 146.6 (triazolylidene), 145.5 (Aryl–C), 140.7 (Aryl–C), 137.4 (Aryl–C), 127.6 (Aryl–C), 123.2 (Aryl–C), 117.0 (Aryl–CH), 111.4 (Aryl–CH), 48.8 (CH_2), 35.2 ($C(CH_3)_3$), 32.3 ($C(CH_3)_3$), 23.4 (CH_2), 22.4 (CH_2), 20.7 (CH_2).

(3,6-Di-*tert*-butyl-1,8-bis-(2,4,5,6-tetrahydropyridin-1,2,3-triazolylidene)-carbazolid) nickel(II) pyridinium tetrafluoridoborate (7). To a solution of **2** (20.0 mg, 33.6 μmol, 1 equiv.) in dichloromethane (5 mL) pyridinium tetrafluoridoborate (16.8 mg, 101 μmol, 3 equiv.) was added, resulting in an immediate colour change to yellow. The solution was concentrated *in vacuo* and filtrated to remove excess pyridinium tetrafluoridoborate. Removal of the remaining solvent gave 7 as yellow solid in quantitative yields. ^1H NMR (C_5D_5N, 298 K, 400 MHz, in ppm): 8.69 (s, 2H, Aryl–H), 8.55 (s, 2H, Aryl–H), 4.38 (s, 4H, CH_2), 1.78 (s, 4H, CH_2), 1.56 (s, 18H, $C(CH_3)_3$), 1.38 (s, 4H, CH_2), 1.24 (s, 4H, CH_2); $^{13}C\{^1H\}$ NMR (C_5D_5N, 298 K, 101 MHz, in ppm): 149.7 (triazolylidene) 143.9 (Aryl–C), 143.8 (Aryl–C), 141.3 (Aryl–C), 136.1 (Aryl–C) 127.9 (Aryl–C),

117.5 (Aryl–CH), 111.7 (Aryl–CH), 48.7 (CH_2), 34.9 ($C(CH_3)_3$), 31.9 ($C(CH_3)_3$), 20.8 (CH_2), 19.3 (CH_2), 19.3 (CH_2); ^{19}F NMR (C_6D_5N, 298 K, 377 MHz, in ppm): −149.9 (BF_4).

3,5-Ditrifluoromethyl-phenylacetylene-(3,6-Di-*tert*-butyl-1,8-bis-(2,4,5,6-tetrahydropyridin-1,2,3-triazolylidene)-carbazol-id) nickel(II) (8). To a solution of **2** (54.0 mg, 84.0 μmol, 1.0 equiv.) in toluene (4 mL) 1-ethynyl-3,5-bis(trifluoromethyl)-benzene (20 mg, 84.0 μmol, 1.0 equiv.) was added under air. After 14 hours at 50 °C the solvent was removed *in vacuo* to yield 99% (68.0 mg, 83.2 μmol) of dark red **8**. ^{1}H NMR (C_6D_6, 298 K, 400 MHz, in ppm): 8.64 (d, J = 1.8 Hz, 2H, Aryl–CH), 8.56 (d, J = 1.8 Hz, 2H, Aryl–CH), 7.98 (s, 2H, acetylide–CH), 7.57 (s, 1H, acetylide–CH), 3.66 (t, J = 6.4 Hz, 4H, CH_2), 3.37 (t, J = 6.4 Hz, 4H, N–CH_2), 1.58 (s, 18H, $C(CH_3)_3$), 1.27 (m, 4H, CH_2), 1.00 (m, 4H, CH_2); $^{13}C\{^1H\}$ NMR (C_6D_6, 298 K, 101 MHz, in ppm): 152.5 (triazolylidene), 145.3 (Aryl–C), 141.5 (Aryl–C), 140.2 (Aryl–C), 138.9 (Aryl–C), 130.0 (acetylide–CH), 124.0 (Aryl–C), 123.1 (acetylide–C), 122.9 (acetylide–C), 117.3 (Aryl–CH), 116.9 (acetylide–CH), 114.3 (alkyne–C), 111.9 (Aryl–CH), 47.4 (N–CH_2), 35.2 ($C(CH_3)_3$), 32.5 ($C(CH_3)_3$), 26.0 (CH_2), 21.9 (CH_2), 20.2 (CH_2); ^{19}F NMR (C_6D_6, 298 K, 377 MHz, in ppm): −62.8 (CF_3).

2,6-Diisopropyl-phenylacetylene-(3,6-di-*tert*-butyl-1,8-bis-(2,4,5,6-tetrahydropyridin-1,2,3-triazolylidene)-carbazolid) nickel(II) (9). To a solution of **2** (35.0 mg, 54.4 μmol, 1 equiv.) in benzene (4 mL) 2-ethinyl-1,3-diisopropyl benzene (15.1 mg, 81.0 μmol, 1.5 equiv.) was added. After refluxing the reaction mixture at 100° C for 24 h all volatiles were removed *in vacuo* to yield 73% (30 mg, 39.4 μmol) of dark red **9**. ^{1}H NMR (C_6D_6, 298 K, 400 MHz, in ppm): 8.62 (d, J = 1.8 Hz, 2H, Aryl–H), 8.50 (d, J = 1.8 Hz, 2H, Aryl–H), 7.21 (d, J = 8.4 Hz, 2H, Dipp-Aryl–CH), 7.13 (m, 1H, Dipp-Aryl–CH), 4.45 (p, J = 6.9 Hz, 2H, i-Pr-CH), 3.77 (t, J = 6.4 Hz, 4H, CH_2), 3.41 (t, J = 6.3 Hz, 4H, N–CH_2), 1.58 (s, 18H, $C(CH_3)_3$), 1.35 (d, J = 7.0 Hz, 12H, i-Pr-CH_3), 1.35 (m, 4H, CH_2), 0.98 (m, 4H, CH_2); $^{13}C\{^1H\}$ NMR (C_6D_6, 298 K, 101 MHz, in ppm): 153.1 (triazolylidene), 148.8 (Dipp-Aryl–C), 145.7 (Aryl–C), 141.5 (Aryl–C), 139.7 (Aryl–C), 139.0 (Aryl–C), 127.5 (Dipp-Aryl–C), 124.6 (Aryl–C), 124.1 (Dipp-Aryl–CH), 122.4 (Dipp-Aryl–CH), 117.0 (Aryl–CH), 113.8 (alkyne–C), 111.7 (Aryl–CH), 47.5 (N–CH_2), 35.2 ($C(CH_3)_3$), 32.6 ($C(CH_3)_3$), 31.8 (i-Pr-CH), 26.8 (CH_2), 24.6 (i-Pr-CH_3), 21.8 (CH_2), 20.6 (CH_2).

Pentafluorophenyl-(3,6-di-*tert*-butyl-1,8-bis-(2,4,5,6-tetrahydropyridin-1,2,3-triazolylidene)-carbazolid) nickel(II) (10). A solution of **2** (20.0 mg, 33.6 μmol, 1 equiv.) in benzene-d_6 (0.6 mL) was treated with pentafluorobenzene (18.2 mg, 101 μmol, 3 equiv.) and refluxed for six days at 120 °C, giving an orange solution. All solvents were removed *in vacuo*, the remaining solid was redissolved in diethyl ether and filtrated to remove remaining starting material. Removal of the solvent yielded 60% (15.0 mg, 20.2 μmol) of **10** as light orange powder. ^{1}H NMR (C_6D_6, 298 K, 400 MHz, in ppm): 8.43 (d, J = 1.6 Hz, 2H, Aryl–CH), 8.31 (d, J = 1.8 Hz, 2H, Aryl–CH), 2.93 (m, 4H, N–CH_2), 1.45 (t, J = 5.9 Hz, 4H, CH_2), 1.36 (s, 18H, $C(CH_3)_3$), 0.43 (m, 8H, CH_2); $^{13}C\{^1H\}$ NMR (C_6D_6, 298 K, 101 MHz, in ppm): 149.2 (triazolylidene), 144.0 (Aryl–C), 141.5 (Aryl–C), 139.9 (Aryl–C), 138.1 (Aryl–C), 124.3 (Aryl–C), 116.9 (Aryl–CH), 112.0 (Aryl–CH), 47.8(N_CH_2), 35.2 ($C(CH_3)_3$), 32.5 ($C(CH_3)_3$), 22.3(CH_2), 20.8(CH_2), 19.8 (CH_2); ^{19}F NMR (C_6D_6, 298 K, 377 MHz, in ppm): −111.2 (m, 2F), −163.1 (tt, J = 20.8, 4.3 Hz, 1F), −164.9 (dddd, J = 30.3, 26.0, 10.8, 5.2 Hz, 2F).

Tetrafluorophenyl-(3,6-di-*tert*-butyl-1,8-bis-(2,4,5,6-tetrahydropyridin-1,2,3-triazolylidene)-carbazolid) nickel(II) (11). A solution of **2** (20.0 mg, 33.6 μmol, 1 equiv.) in benzene-d_6 (0.6 mL) was treated with tetrafluorobenzene (15.1 mg, 101 μmol, 3 equiv.) and refluxed for six days at 120 °C, giving an orange solution. All solvents were removed *in vacuo*, the remaining solid was redissolved in diethylether and filtrated to remove remaining starting material. Removal of the solvent yielded 65% (16.0 mg, 21.8 μmol) of **11** as light orange powder. ^{1}H NMR (C_6D_6, 298 K, 400 MHz, in ppm): 8.66 (d, J = 1.7 Hz, 2H, Aryl–CH), 8.54 (d, J = 1.7 Hz, 2H, Aryl–CH), 6.74 (m, 1H, PhF_4-CH), 3.19 (t, J = 6.1 Hz, 4H, N–CH_2), 1.73 (m, 4H, CH_2), 1.59 (s, 18H, ($C(CH_3)_3$)), 0.71 (m, 8H, CH_2); $^{13}C\{^1H\}$ NMR (C_6D_6, 298 K, 101 MHz, in ppm): 149.6 (triazolylidene), 144.2 (Aryl–C), 141.5 (Aryl–C), 139.8 (Aryl–C), 138.2 (Aryl–C), 124.4 (Aryl–C), 116.9 (Aryl–CH), 112.0 (Aryl–CH), 100.1 (PhF_4-CH), 47.8 (N–CH_2), 35.2 ($C(CH_3)_3$), 32.6 ($C(CH_3)_3$), 22.1 (CH_2), 20.8 (CH_2), 20.1 (CH_2). ^{19}F NMR (C_6D_6, 298 K, 377 MHz, in ppm): −113.3 (ddd, J = 33.8, 15.6, 6.9 Hz, 2F), −142.8 (ddt, J = 25.1, 15.6, 9.1 Hz, 2F).

(3,6-Di-*tert*-butyl-1,8-bis-(2,4,5,6-tetrahydropyridin-1,2,3-triazolylidene)-carbazolid) nickel(II) ethanone enolate (12). To a solution of **2** (50.0 mg, 83.9 μmol, 1 equiv.) in benzene (6 mL) molecular sieves and diphenylethanone (16.4 mg, 83.9 μmol, 1 equiv.) were added. After stirring the dark red reaction mixture at 120 °C in an argon atmosphere for two days colour change to dark orange was observed. The mixture was concentrated to 1 mL *in vacuo* and pentante (6 mL) was added. The resulting suspension was filtrated to give a clear, light orange solution. Removal of all volatiles *in vacuo* yielded 46% (30.0 mg, 38.6 μmol) of **12** as dark orange powder. ^{1}H NMR (C_6D_6, 298 K, 400 MHz, in ppm): 8.83 (dd, J = 8.3, 1.3 Hz, 2H, ethanone–Ph–CH), 8.52 (d, J = 1.8 Hz, 2H, Aryl–CH), 8.35 (d, J = 1.8 Hz, 2H, Aryl–CH), 8.25 (dd, J = 8.4, 1.4 Hz, 2H, ethanone–Ph–CH), 7.47 (m, 2H, ethanone–Ph–CH), 7.12 (m, 1H, ethanone–Ph–CH), 6.95 (m, 2H, ethanone–Ph–CH), 6.73 (tt, J = 7.0, 1.3 Hz, 1H, ethanone–Ph–CH), 5.91 (s, 1H, ethanone–CH), 3.57 (t, J = 6.3 Hz, 4H, CH_2), 3.33 (t, J = 6.3 Hz, 4H, N–CH_2), 1.50 (s, 18H, $C(CH_3)_3$), 1.10 (m, 4H, CH_2), 0.94 (m, 4H, CH_2); $^{13}C\{^1H\}$ NMR (C_6D_6, 298 K, 101 MHz, in ppm): 169.7 (ethanone–C═O), 149.2 (ethanone–Ph–C), 147.2 (triazolylidene), 144.8 (Aryl–C), 142.8 (ethenone–Ph–C), 141.5 (Aryl–C), 139.9 (Aryl–C), 138.0 (Aryl–C), 127.3 (ethanone–Ph–CH), 127.0 (ethanone–Ph–CH), 126.2 (ethanone–Ph–CH), 123.7 (Aryl–C), 121.8 (ethanone–Ph–C), 116.8 (Aryl–CH), 111.4 (Aryl–CH), 102.2 (ethanone–CH), 47.6 (N–CH_2), 35.0 ($C(CH_3)_3$), 32.4 ($C(CH_3)_3$), 23.1(CH_2), 21.5 (CH_2), 19.9 (CH_2).

(3,6-Di-*tert*-butyl-1,8-bis-(2,4,5,6-tetrahydropyridin-1,2,3-triazolylidene)-carbazolid) nickel(II) 1,5-dimethoxy-2-(methoxycarbonyl)-1,5-dioxopent-2-en-3-olate (13). To a solution of **2** (25.0 mg, 42.0 μmol, 1 equiv.) in benzene (4 mL) malonic acid

dimethyl ester (8.3 mg, 63.0 μmol, 1.5 equiv.) was added in an argon atmosphere. After stirring the reaction mixture for two hours at 120 °C the colour changed from red to a light orange. All volatiles were removed *in vacuo*, recrystallisation *via* evaporation from a concentrated solution in diethyl ether yielded 59% (20 mg, 24.7 μmol) of dark orange **13**. ^{1}H NMR (C_6D_6, 298 K, 400 MHz, in ppm): 8.58 (d, J = 1.8 Hz, 2H, Aryl–CH), 8.37 (d, J = 1.8 Hz, 2H, Aryl–CH), 6.08 (s, 2H, malonate–CH_2), 3.77 (s, 3H, OMe), 3.51 (s, 3H, OMe), 3.43 (m, 8H, CH_2), 3.04 (s, 3H, OMe), 1.51 (s, 18H, $C(CH_3)_3$), 1.24 (m, 4H, CH_2), 1.14 (m, 4H, CH_2); $^{13}C\{^{1}H\}$ NMR (C_6D_6, 298 K, 101 MHz, in ppm): 180.9 (CO), 170.0 (CO), 168.6 (CO), 145.9 (triazolylidene), 144.6 (Aryl–C), 141.5 (Aryl–C), 140.5 (Aryl–C), 137.8 (Aryl–C), 123.6 (Aryl–C), 117.0 (Aryl–CH), 111.6 (Aryl–CH), 102.1 (malonate–C), 50.9 (OMe), 50.8 (OMe), 50.3 (OMe), 49.8 (malonate–CH_2), 47.7 (CH_2), 35.1 ($C(CH_3)_3$), 32.4 ($C(CH_3)_3$), 23.7 (CH_2), 21.5 (CH_2), 20.0 (CH_2).

(3,6-Di-*tert*-butyl-1,8-bis-(2,4,5,6-tetrahydropyridin-1,2,3-triazolylidene)-carbazolid) nickel(II) cyanide (14). Method A: a solution of **2** (100 mg, 168 μmol) in acetonitrile (100 mL) was left at room temperature under air for three days. A colour change to bright orange was observed, removal of all volatiles *in vacuo* yielded 85% (86.5 mg, 142.8 μmol) of **14**. Method B: a solution of **1** (50 mg, 83.9 μmol, 1 equiv.) in dichloromethane was treated with an aqueous solution of potassium cyanide (1 M, 20 mL) and stirred for 15 minutes under air. The orange organic phase was dried over sodium sulfate and the solvent was removed *in vacuo* to yield 79% of **14** (40 mg, 66.1 μmol). ^{1}H NMR (C_6D_6, 298 K, 400 MHz, in ppm): 8.63 (d, J = 1.8 Hz, 2H, Aryl–CH), 8.55 (d, J = 1.8 Hz, 2H, Aryl–CH), 3.83 (t, J = 6.5 Hz, 4H, CH_2), 3.34 (t, J = 6.3 Hz, 4H, N–CH_2), 1.57 (s, 18H ($C(CH_3)_3$)), 1.25 (m, 4H, CH_2), 1.01 (m, 4H, CH_2); $^{13}C\{^{1}H\}$ NMR (C_6D_6, 298 K, 101 MHz, in ppm): 150.1 (triazolylidene), 145.7 (Aryl–C), 141.5 (Aryl–C), 140.4 (Aryl–C), 138.5 (Aryl–C), 123.9 (Aryl–C), 117.2 (Aryl–CH), 112.0 (Aryl–CH), 47.6 (N–CH_2), 35.2, 32.5, 26.2 (CH_2), 21.7 (CH_2), 20.0 (CH_2). ATR-IR (cm^{-1}) = 2107.

X-ray crystallography details. Intensity data of single crystals of the investigated compounds were collected using MoK_α irradiation (λ = 0.71073 Å) either on a Bruker D8 Quest or a Rigaku Synergy DW rotating anode diffractometer. All hydrogen atoms were placed in positions of optimized geometry, unless being bound to a heteroatom (compounds **2** and **5**). The isotropic displacement parameters of all hydrogen atoms were tied to those of their corresponding carrier atoms by a factor of 1.2 or 1.5. All non-hydrogen atoms were refined anisotropically. Data were corrected for Lorentz and polarization effects; semiempirical absorption corrections were performed on the basis of multiple scans using SADABS.[56] The structures were solved by direct methods using SHELXT.[57] The structures were refined by full-matrix least-squares procedures on F^2 using ShelXL[58] in the graphical interface of OLEX2.[59] The latter was also used to prepare material for publication. SQUEEZE[60] was used to "delete" residual electron density from highly disordered and thus hardly refinable solvent molecules in the structures of **5** (2 C_6H_6), **8** (2 C_7H_8), **11** (1.6 C_6H_6) and **12′** (2 C_6H_6).

Conflicts of interest

There are no conflicts to declare.

Acknowledgements

We thank the University of Innsbruck for funding of this work. The computational results presented here have been achieved using the LEO HPC infrastructure at the University of Innsbruck.

References

1 (*a*) D. J. Nelson and S. P. Nolan, *Coord. Chem. Rev.*, 2017, **353**, 278–294; (*b*) R. Jira, *Angew. Chem., Int. Ed.*, 2009, **48**, 9034–9037; (*c*) J. A. Keith and P. M. Henry, *Angew. Chem., Int. Ed.*, 2009, **48**, 9038–9049.
2 H. E. Bryndza and W. Tam, *Chem. Rev.*, 1988, **88**, 1163–1188.
3 J. R. Fulton, A. W. Holland, D. J. Fox and R. G. Bergman, *Acc. Chem. Res.*, 2002, **35**, 44–56.
4 H. W. Roesky, S. Singh, K. K. M. Yusuff, J. A. Maguire and N. S. Hosmane, *Chem. Rev.*, 2006, **106**, 3813–3843.
5 A. S. Romanov and M. Bochmann, *Organometallics*, 2015, **34**, 2439–2454.
6 G. R. Fulmer, A. N. Herndon, W. Kaminsky, R. A. Kemp and K. I. Goldberg, *J. Am. Chem. Soc.*, 2011, **133**, 17713–17726.
7 D.-A. Roşca, D. A. Smith and M. Bochmann, *Chem. Commun.*, 2012, **48**, 7247–7249.
8 (*a*) H. Brombacher and H. Vahrenkamp, *Inorg. Chem.*, 2004, **43**, 6042–6049; (*b*) H. Brombacher and H. Vahrenkamp, *Inorg. Chem.*, 2004, **43**, 6050–6053; (*c*) L. M. Martínez-Prieto, P. Palma, E. Álvarez and J. Cámpora, *Inorg. Chem.*, 2017, **56**, 13086–13099.
9 (*a*) D. Dhar and W. B. Tolman, *J. Am. Chem. Soc.*, 2015, **137**, 1322–1329; (*b*) B. Liu, B. Liu, Y. Zhou and W. Chen, *Organometallics*, 2010, **29**, 1457–1464; (*c*) G. C. Fortman, A. M. Z. Slawin and S. P. Nolan, *Organometallics*, 2010, **29**, 3966–3972.
10 H. Ibrahim, R. Guillot, F. Cisnetti and A. Gautier, *Chem. Commun.*, 2014, **50**, 7154–7156.
11 S. Bagherzadeh and N. P. Mankad, *Chem. Commun.*, 2018, **54**, 1097–1100.
12 (*a*) J. Cámpora, P. Palma, D. del Río and E. Álvarez, *Organometallics*, 2004, **23**, 1652–1655; (*b*) J. M. van Middlesworth and S. A. Wood, *Geochim. Cosmochim. Acta*, 1999, **63**, 1751–1765; (*c*) I. Nakajima, M. Shimizu, Y. Okuda, R. Akiyama, R. Tadano, M. Nagaoka, N. Uemura, Y. Yoshida, T. Mino, H. Shinozaki and T. Yamamoto, *Adv. Synth. Catal.*, 2022, **364**, 1763–1768.
13 (*a*) T. G. Appleton, J. R. Hall, S. F. Ralph and C. S. M. Thompson, *Inorg. Chem.*, 1984, **23**, 3521–3525; (*b*) G. W. Bushnell, K. R. Dixon, R. G. Hunter and J. J. McFarland, *Can. J. Chem.*, 1972, **50**, 3694–3699;

(*c*) T. L. Lohr, W. E. Piers and M. Parvez, CCDC 891234: Experimental Crystal Structure Determination, 2012.

14 Please note that the references given for the single metals are only a selection of examples and do not represent a complete overview of late transition metal hydroxide complexes reported.

15 G. Lopez, G. Garcia, G. Sanchez, J. Garcia, J. Ruiz, J. A. Hermoso, A. Vegas and M. Martinez-Ripoll, *Inorg. Chem.*, 1992, **31**, 1518–1523.

16 J. Cámpora, I. Matas, P. Palma, C. Graiff and A. Tiripicchio, *Organometallics*, 2005, **24**, 2827–2830.

17 D. Adhikari, S. Mossin, F. Basuli, B. R. Dible, M. Chipara, H. Fan, J. C. Huffman, K. Meyer and D. J. Mindiola, *Inorg. Chem.*, 2008, **47**, 10479–10490.

18 A. Castonguay, A. L. Beauchamp and D. Zargarian, *Inorg. Chem.*, 2009, **48**, 3177–3184.

19 D. Powell-Jia, J. W. Ziller, A. G. Dipasquale, A. L. Rheingold and A. S. Borovik, *Dalton Trans.*, 2009, 2986–2992.

20 M. K. Samantaray, M. M. Shaikh and P. Ghosh, *Organometallics*, 2009, **28**, 2267–2275.

21 J. Borau-Garcia, D. V. Gutsulyak, R. J. Burford and W. E. Piers, *Dalton Trans.*, 2015, **44**, 12082–12085.

22 D. Huang and R. H. Holm, *J. Am. Chem. Soc.*, 2010, **132**, 4693–4701.

23 D. Huang, O. V. Makhlynets, L. L. Tan, S. C. Lee, E. V. Rybak-Akimova and R. H. Holm, *Inorg. Chem.*, 2011, **50**, 10070–10081.

24 K. J. Jonasson, A. H. Mousa and O. F. Wendt, *Polyhedron*, 2018, **143**, 132–137.

25 C. Yao, P. Chakraborty, E. Aresu, H. Li, C. Guan, C. Zhou, L.-C. Liang and K.-W. Huang, *Dalton Trans.*, 2018, **47**, 16057–16065.

26 T. J. Schmeier, A. Nova, N. Hazari and F. Maseras, *Chem. – Eur. J.*, 2012, **18**, 6915–6927.

27 F. Schneck, J. Ahrens, M. Finger, A. C. Stückl, C. Würtele, D. Schwarzer and S. Schneider, *Nat. Commun.*, 2018, **9**, 1161.

28 K. Tomomatsu, Y. Yamada, Y. Koga and K. Matsubara, *Chem. Lett.*, 2022, **51**, 836–839.

29 J. Rajpurohit, P. Shukla, P. Kumar, C. Das, S. Vaidya, M. Sundararajan, M. Shanmugam and M. Shanmugam, *Inorg. Chem.*, 2019, **58**, 6257–6267.

30 P. Pinter, C. M. Schüßlbauer, F. A. Watt, N. Dickmann, R. Herbst-Irmer, B. Morgenstern, A. Grünwald, T. Ullrich, M. Zimmer, S. Hohloch, D. M. Guldi and D. Munz, *Chem. Sci.*, 2021, **12**, 7401–7410.

31 B. Wittwer, N. Dickmann, S. Berg, D. Leitner, L. Tesi, D. Hunger, R. Gratzl, J. van Slageren, N. I. Neuman, D. Munz and S. Hohloch, *Chem. Commun.*, 2022, **58**, 6096–6099.

32 F. A. Watt, B. Sieland, N. Dickmann, R. Schoch, R. Herbst-Irmer, H. Ott, J. Paradies, D. Kuckling and S. Hohloch, *Dalton Trans.*, 2021, **50**, 17361–17371.

33 (*a*) P. Dierks, A. Kruse, O. S. Bokareva, M. J. Al-Marri, J. Kalmbach, M. Baltrun, A. Neuba, R. Schoch, S. Hohloch, K. Heinze, M. Seitz, O. Kühn, S. Lochbrunner and M. Bauer, *Chem. Commun.*, 2021, **57**, 6640–6643; (*b*) S. Hohloch, B. Sarkar, L. Nauton, F. Cisnetti and A. Gautier, *Tetrahedron Lett.*, 2013, **54**, 1808–1812; (*c*) S. Hohloch, C.-Y. Su and B. Sarkar, *Eur. J. Inorg. Chem.*, 2011, **2011**, 3067–3075; (*d*) R. Maity, A. Verma, M. van der Meer, S. Hohloch and B. Sarkar, *Eur. J. Inorg. Chem.*, 2016, **2016**, 111–117; (*e*) M. Rigo, L. Hettmanczyk, F. J. L. Heutz, S. Hohloch, M. Lutz, B. Sarkar and C. Müller, *Dalton Trans.*, 2016, **46**, 86–95; (*f*) L. Suntrup, S. Hohloch and B. Sarkar, *Chem. – Eur. J.*, 2016, **22**, 18009–18018; (*g*) S. Bertini, M. Rahaman, A. Dutta, P. Schollhammer, A. V. Rudnev, F. Gloaguen, P. Broekmann and M. Albrecht, *Green Chem.*, 2021, **23**, 3365–3373.

34 T.-Y. Lee, Y.-J. Lin, Y.-Z. Chang, L.-S. Huang, B.-T. Ko and J.-H. Huang, *Organometallics*, 2017, **36**, 291–297.

35 L. Yang, D. R. Powell and R. P. Houser, *Dalton Trans.*, 2007, 955–964.

36 (*a*) J. Ghannam, Z. Sun, T. R. Cundari, M. Zeller, A. Lugosan, C. M. Stanek and W.-T. Lee, *Inorg. Chem.*, 2019, **58**, 7131–7135; (*b*) J. Ghannam, T. Al Assil, T. C. Pankratz, R. L. Lord, M. Zeller and W.-T. Lee, *Inorg. Chem.*, 2018, **57**, 8307–8316.

37 (*a*) P. Zimmermann, D. Ar, M. Rößler, P. Holze, B. Cula, C. Herwig and C. Limberg, *Angew. Chem., Int. Ed.*, 2021, **60**, 2312–2321; (*b*) D. Huang, L. Deng, J. Sun and R. H. Holm, *Inorg. Chem.*, 2009, **48**, 6159–6166.

38 (*a*) N. J. Hartmann, G. Wu and T. W. Hayton, *Angew. Chem., Int. Ed.*, 2015, **54**, 14956–14959; (*b*) M. S. Varonka and T. H. Warren, *Organometallics*, 2010, **29**, 717–720; (*c*) J. Cho, G. P. A. Yap and C. G. Riordan, *Inorg. Chem.*, 2007, **46**, 11308–11315.

39 (*a*) J. Davies, D. Janssen-Müller, D. P. Zimin, C. S. Day, T. Yanagi, J. Elfert and R. Martin, *J. Am. Chem. Soc.*, 2021, **143**, 4949–4954; (*b*) S. Liang, S. Chattopadhyay, J. L. Petersen, V. G. Young and M. P. Jensen, *Polyhedron*, 2013, **50**, 75–81; (*c*) C. M. Simon, S. L. Dudra, R. T. McGuire, M. J. Ferguson, E. R. Johnson and M. Stradiotto, *ACS Catal.*, 2022, **12**, 1475–1480.

40 (*a*) N. M. Camasso and M. S. Sanford, *Science*, 2015, **347**, 1218–1220; (*b*) J. B. Diccianni and T. Diao, *Trends Chem.*, 2019, **1**, 830–844; (*c*) Y. Li, Y. Luo, L. Peng, Y. Li, B. Zhao, W. Wang, H. Pang, Y. Deng, R. Bai, Y. Lan and G. Yin, *Nat. Commun.*, 2020, **11**, 417; (*d*) K. E. Poremba, S. E. Dibrell and S. E. Reisman, *ACS Catal.*, 2020, **10**, 8237–8246; (*e*) R. Pothiraja, A. Milanov, H. Parala, M. Winter, R. A. Fischer and A. Devi, *Dalton Trans.*, 2009, 654–663; (*f*) S. Z. Tasker, E. A. Standley and T. F. Jamison, *Nature*, 2014, **509**, 299–309.

41 For an overview of pK_a value of the substrates used, please see: (*a*) K. Shen, Y. Fu, J.-N. Li, L. Liu and Q.-X. Guo, *Tetrahedron*, 2007, **63**, 1568–1576; (*b*) **https://organicchemistry-data.org/hansreich/resources/pka/pka_data/evans_pKa_table.pdf**.

42 (*a*) D. Gallego, A. Brück, E. Irran, F. Meier, M. Kaupp, M. Driess and J. F. Hartwig, *J. Am. Chem. Soc.*, 2013, **135**,

15617–15626; (*b*) L. F. Groux and D. Zargarian, *Organometallics*, 2003, **22**, 4759–4769; (*c*) W. M. Khairul, M. A. Fox, N. N. Zaitseva, M. Gaudio, D. S. Yufit, B. W. Skelton, A. H. White, J. A. K. Howard, M. I. Bruce and P. J. Low, *Dalton Trans.*, 2009, 610–620; (*d*) H.-F. Klein, M. Zwiener, A. Petermann, T. Jung, G. Cordier, B. Hammerschmitt, U. Flörke, H.-J. Haupt and Y. Dartiguenave, *Chem. Ber.*, 1994, **127**, 1569–1578; (*e*) A. H. Mousa, J. Bendix and O. F. Wendt, *Organometallics*, 2018, **37**, 2581–2593; (*f*) P. M. Pérez García, P. Ren, R. Scopelliti and X. Hu, *ACS Catal.*, 2015, **5**, 1164–1171; (*g*) S. F. Tyler, S. N. Natoli, B. Vlaisavljevich, P. E. Fanwick and T. Ren, *Inorg. Chem.*, 2015, **54**, 10058–10064; (*h*) G. L. O. Wilson, M. Abraha, J. A. Krause and H. Guan, *Dalton Trans.*, 2015, **44**, 12128–12136; (*i*) X. Zhang, Di Qi, C. Jiao, X. Liu and G. Zhang, *Nat. Commun.*, 2021, **12**, 4904; (*j*) A. B. Salah and D. Zargarian, *Dalton Trans.*, 2011, **40**, 8977–8985.

43 T. Schaub, P. Fischer, T. Meins and U. Radius, *Eur. J. Inorg. Chem.*, 2011, **2011**, 3122–3126.

44 (*a*) J. A. Hatnean, R. Beck, J. D. Borrelli and S. A. Johnson, *Organometallics*, 2010, **29**, 6077–6091; (*b*) Y. Minami, H. Yoshiyasu, Y. Nakao and T. Hiyama, *Angew. Chem., Int. Ed.*, 2013, **52**, 883–887.

45 A. J. Nett, W. Zhao, P. M. Zimmerman and J. Montgomery, *J. Am. Chem. Soc.*, 2015, **137**, 7636–7639.

46 M. W. Kuntze-Fechner, H. Verplancke, L. Tendera, M. Diefenbach, I. Krummenacher, H. Braunschweig, T. B. Marder, M. C. Holthausen and U. Radius, *Chem. Sci.*, 2020, **11**, 11009–11023.

47 (*a*) M. R. Churchill, K. L. Kalra and M. V. Veidis, *Inorg. Chem.*, 1973, **12**, 1656–1662; (*b*) J. Ponce-de-León, E. Gioria, J. M. Martínez-Ilarduya and P. Espinet, *Inorg. Chem.*, 2020, **59**, 18287–18294; (*c*) S. Sabater, M. J. Page, M. F. Mahon and M. K. Whittlesey, *Organometallics*, 2017, **36**, 1776–1783; (*d*) G. Sánchez, F. Ruiz, J. L. Serrano, M. C. R. de Arellano and G. López, *Eur. J. Inorg. Chem.*, 2000, **2000**, 2185–2191; (*e*) J. Forniés, A. Martín, L. F. Martín, B. Menjón, H. A. Kalamarides, L. F. Rhodes, C. S. Day and V. W. Day, *Chem. – Eur. J.*, 2002, **8**, 4925–4934.

48 (*a*) S. A. Johnson, E. T. Taylor and S. J. Cruise, *Organometallics*, 2009, **28**, 3842–3855; (*b*) S. A. Johnson, N. M. Mroz, R. Valdizon and S. Murray, *Organometallics*, 2011, **30**, 441–457; (*c*) S. A. Johnson, C. W. Huff, F. Mustafa and M. Saliba, *J. Am. Chem. Soc.*, 2008, **130**, 17278–17280; (*d*) J. A. Hatnean and S. A. Johnson, *Organometallics*, 2012, **31**, 1361–1373; (*e*) D. A. Baird, S. Jamal and S. A. Johnson, *Organometallics*, 2017, **36**, 1436–1446.

49 (*a*) A. L. Keen and S. A. Johnson, *J. Am. Chem. Soc.*, 2006, **128**, 1806–1807; (*b*) A. L. Keen, M. Doster and S. A. Johnson, *J. Am. Chem. Soc.*, 2007, **129**, 810–819.

50 (*a*) C.-N. Chen, W.-M. Cheng, J.-K. Wang, T.-H. Chao, M.-J. Cheng and R.-S. Liu, *Angew. Chem., Int. Ed.*, 2021, **60**, 4479–4484; (*b*) D. Matković-Čalogović, *Acta Crystallogr., Sect. C: Cryst. Struct. Commun.*, 1987, **43**, 1473–1475; (*c*) J. Vicente, M.-T. Chicote, I. Saura-Llamas and M.-C. Lagunas, *J. Chem. Soc., Chem. Commun.*, 1992, 915.

51 (*a*) M. J. Carney, P. J. Walsh, F. J. Hollander and R. G. Bergman, *Organometallics*, 1992, **11**, 761–777; (*b*) G. E. Leroi and W. Klemperer, *J. Chem. Phys.*, 1961, **35**, 774–775.

52 (*a*) G. Urgoitia, R. SanMartin, M. T. Herrero and E. Domínguez, *Chem. Commun.*, 2015, **51**, 4799–4802; (*b*) X. Wang, R.-X. Chen, Z.-F. Wei, C.-Y. Zhang, H.-Y. Tu and A.-D. Zhang, *J. Org. Chem.*, 2016, **81**, 238–249.

53 T. Komnenos, *Chem. Mon.*, 1910, **31**, 421–438.

54 Q.-X. Liu, F.-B. Xu, Q.-S. Li, H.-B. Song and Z.-Z. Zhang, *Organometallics*, 2004, **23**, 610–614.

55 J. J. Garcia and W. D. Jones, *Organometallics*, 2000, **19**, 5544–5545.

56 L. Krause, R. Herbst-Irmer, G. M. Sheldrick and D. Stalke, *J. Appl. Crystallogr.*, 2015, **48**, 3–10.

57 G. M. Sheldrick, *Acta Crystallogr., Sect. A: Found. Adv.*, 2015, **71**, 3–8.

58 (*a*) G. M. Sheldrick, *Acta Crystallogr., Sect. A: Found. Crystallogr.*, 2015, **71**, 3–8; (*b*) G. M. Sheldrick, *Acta Crystallogr., Sect. A: Found. Crystallogr.*, 2008, **64**, 112–122.

59 O. V. Dolomanov, L. J. Bourhis, R. J. Gildea, J. A. K. Howard and H. Puschmann, *Appl. Crystallogr.*, 2009, **42**, 339–341.

60 A. L. Spek, *Acta Crystallogr., Sect. A: Found. Crystallogr.*, 2015, **71**, 9–18.